P-ISSN: 3050-9734
E-ISSN: 3050-9742
EUROPEAN ADVANCED JOURNAL FOR EMERGING TECHNOLOGIES
EAJET
VOLUME: 03 ISSUE: 03
RECEIVED: APRIL 21 REVISED: MAY 19 ACCEPTED: JUNE 28 PUBLISHED: JULY 11

Experimental and Machine Learning Approaches for Discharge Estimation in Arched Labyrinth Weirs

Ajmal Hussain [1], Mujib Ansari [2], Mohd Danish [3] and Hazi Azamathulla [4,*]

[1] Assistant Professor, Department of Civil Engineering, Zakir Husain College of Engineering and Technology, Aligarh Muslim University, Aligarh, 202002, U.P., India.

[2] Professor, Department of Civil Engineering, Zakir Husain College of Engineering and Technology, Aligarh Muslim University, Aligarh, 202002, U.P., India.

[3] Assistant Professor, Civil Engineering Section, University Polytechnic, Aligarh Muslim University, Aligarh, 202002, U.P., India. ORCID: https://orcid.org/0000-0002-7118-1131

[4] Professor of Hydraulic Engineering, Department of Civil and Environmental Engineering, University of the West Indies, St. Augustine, Trinidad.

* **Correspondence:** azmatheditor@gmail.com

Abstract: A weir is a hydraulic structure installed across or parallel to an open channel to regulate or measure flow discharge. Weirs are classified based on shape, discharge characteristics, crest width, and crest type. Among these, the arched labyrinth weir is characterized by its extended crest length, achieved through arching and notches, which enhances its hydraulic efficiency. This study presents a comprehensive analytical and experimental investigation into the discharge characteristics of arched labyrinth weirs in open channels. The artificial neural network model demonstrated exceptional predictive performance, achieving a mean squared error of 2.84×10^{-7}, a mean absolute percentage error of 0.000191, and a correlation coefficient approaching 1, highlighting its accuracy and reliability in discharge estimation.

Keywords: Labyrinth weir, Coefficient of discharge, Froude number, Artificial Neural Network

Graphical Abstract

P-ISSN: 3050-9734
E-ISSN: 3050-9742
EUROPEAN ADVANCED JOURNAL FOR EMERGING TECHNOLOGIES
VOLUME: 03 ISSUE: 03
RECEIVED: APRIL 21 REVISED: MAY 19 ACCEPTED: JUNE 28 PUBLISHED: JULY 11

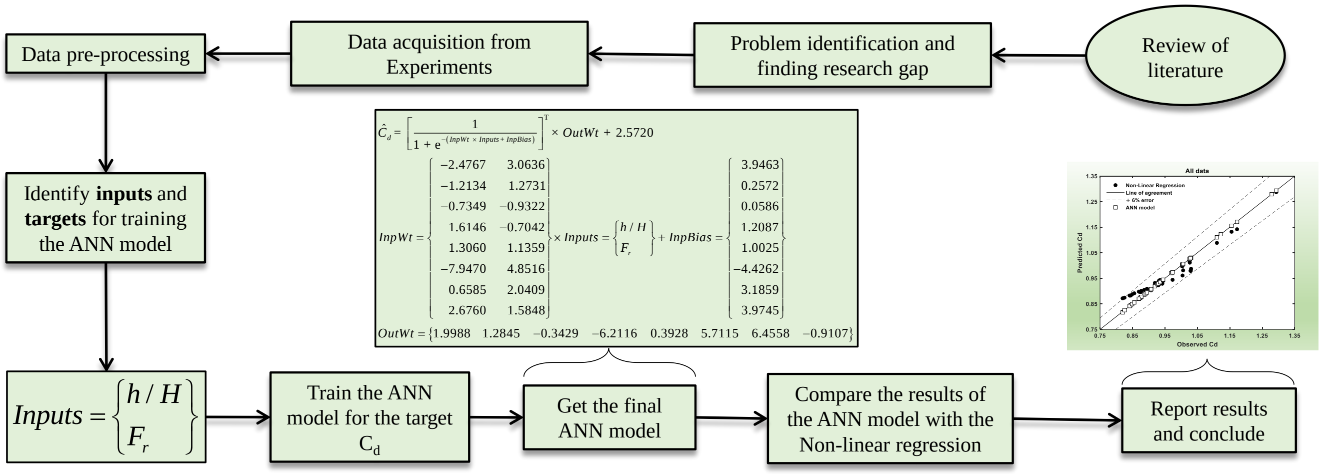

List of symbols

B	width of the main channel
C_d	coefficient of discharge
D	orifice crest height
$F_r = V/(gy)^{0.5}$	Froude number
g	acceleration due to gravity
h	depth of water over the crest of arched labyrinth weir
H	crest height of arched labyrinth weir
L	parametric crest length of the arched labyrinth weir
Q	discharge through the labyrinth weir
$R_e = (\rho\ V\ B)/\mu$	Reynolds number
V	velocity of flow over the cross section of the basin
y	depth of water in the channel
μ	dynamic viscosity of water
ρ	density of water

1. Introduction

A labyrinth weir is an advanced hydraulic control structure featuring a folded or serpentine configuration to increase the effective crest length. This design significantly enhances

P-ISSN: 3050-9734 E-ISSN: 3050-9742

EUROPEAN ADVANCED JOURNAL FOR EMERGING TECHNOLOGIES

EAJET

VOLUME: 03 ISSUE: 03

RECEIVED: APRIL 21 REVISED: MAY 19 ACCEPTED: JUNE 28 PUBLISHED: JULY 11

discharge capacity compared to conventional linear overflow structures while maintaining the same channel width and upstream head conditions. Primarily employed as spillways for dams with width limitations, labyrinth weirs have received significant attention in recent hydrological research, highlighting the critical influence of geometric parameters on their hydraulic performance. While previous studies have contributed to improving the design principles of these weirs, their optimal configuration remains reliant on empirically derived models and performance evaluations. The discharge capacity of a labyrinth weir is strongly dependent on its crest length and other governing parameters, making it a widely adopted solution for flow regulation. Labyrinth weirs are a preferred alternative for enhancing discharge capacity and maintaining upstream water levels. Notably, implementing an arced cycle configuration in reservoir applications has been shown to optimize flow orientation, thereby increasing discharge efficiency. Research findings suggest that arced labyrinth weirs can achieve up to a 4.5% improvement in efficiency compared to traditional linear designs. Moreover, labyrinth weirs with a greater number of smaller cycles have been found to be more efficient and cost-effective than those with fewer cycles of equivalent total length. The hydraulic performance and discharge capacity of labyrinth weirs are influenced by multiple factors, including aspect ratio, sidewall angle, channel conditions, and various geometric parameters inherent to the weir structure. Optimizing these design elements is crucial for maximizing flow efficiency while maintaining structural and economic feasibility (Ansari et al., 2021; Sangsefidi et al., 2018).

Numerous studies have assessed the discharge capacity across labyrinth weirs featuring diverse crest shapes, underscoring the versatility and adaptability of these hydraulic structures. However, a predominant trend emerges where investigations have traditionally focused on individual cases without comprehensive comparisons between various crest shapes (Crookston, 2010; Crookston & Tullis, 2012, 2013; Darvas, 1971; Hay & Taylor, 1970; Houston, 1982; Lux, 1984; Savage et al., 2004; Taylor, 1968; B. P. Tullis et al., 2007). Notably, Amanian, (1987) highlighted the superior efficacy of quarter-round crest configurations. In contrast, J. P. Tullis et al., (1995) observed that half-round crests exhibited more significant discharge coefficients under low heads but lower coefficients under high heads than quarter-round configurations. Several studies have proposed equations for calculating the head-discharge relationship in labyrinth weirs, implying that the discharge coefficient may be independent of the specific crest geometry (Ghodsian, 2009). Similarly, Khode & Tembhurkar, (2010) advocated for quarter-round crests. Introducing the concept of nappe interference, Crookston & Tullis, (2012) elucidated nappe aeration and flow dynamics, offering parametric methodologies for estimating nappe interference size contingent upon labyrinth weir crest shapes. Subsequent studies by Crookston & Tullis, (2013) substantiated slight enhancements in efficiency and discharge capacity under low-flow conditions for half-round crests while delineating the ogee-type crest as a modified half-round variant. Idrees et al., (2016) utilized round crests to explore discharge coefficient, presenting empirical formulations for coefficient calculation. Furthermore, Bilhan & Emiroglu, (2016) experimentally determined discharge coefficients for semi-circular and trapezoidal labyrinth weirs with sharp crests, revealing nuanced performance variations across crest shapes. Idrees & Al-Ameri, (2022) extended these investigations to compound labyrinth weirs with flat crests, observing negligible discrepancies in coefficient values compared to conventional labyrinth weir orientations. Idrees et al., (2018) investigated discharge coefficient behaviors for compound labyrinth weirs employing half-round crests, offering predictive equations spanning sidewall angles ranging from 6 to 9 degrees. Yousif & Karakouzian, (2020) carry out an experimental study into flat-crested rectangular labyrinth weirs, revealing the role of corner configuration in influencing discharge capacity. Building upon this research, Idrees & Al-Ameri, (2022) employed a half-round crest configuration within a compound labyrinth weir to mitigate pressure beneath the nappe flow, advocating for artificial ventilation techniques to augment discharge coefficients. Comparative analysis between vent pipe systems and suction devices showcased the superior efficacy of artificial aeration in reducing pressure behind the nappe flow. Additionally, Hussain et al., (2022) investigated flow characteristics over triangular labyrinth weirs utilizing sharp crest profiles, identifying weir height and vertex angle as primary factors influencing the discharge coefficient. In a novel advancement, Idrees & Al-Ameri, (2023b) proposed modifications to labyrinth weir structures, integrating quarter-round crest profiles and sidewall angle adjustments to enhance hydraulic performance. Recently, labyrinth weirs combined with stepped chutes were also proposed (Crookston et al., 2024).

This study presents a series of laboratory experiments conducted under free-flow conditions using a sharp-crested arched labyrinth weir. The experimental data were employed to develop a discharge coefficient (C_d) estimation model using conventional regression

P-ISSN: 3050-9734
E-ISSN: 3050-9742
EUROPEAN ADVANCED JOURNAL FOR EMERGING TECHNOLOGIES
EAJET
VOLUME: 03 ISSUE: 03
RECEIVED: APRIL 21 REVISED: MAY 19 ACCEPTED: JUNE 28 PUBLISHED: JULY 11

techniques. Additionally, a predictive model was developed utilizing an Artificial Neural Network (ANN) to enhance the accuracy of C_d estimation specifically for arched labyrinth weirs. A comparative analysis was performed to evaluate the predictive performance of the developed ANN model against the conventional regression approach.

2. Dimensional Analysis

For the arched labyrinth weir, the discharge, Q can be calculated by Equation (1).

$$Q = \frac{2}{3} C_d \sqrt{g} L h^{3/2} \quad (1)$$

The dimensional analysis was performed using the Buckingham pi method to obtain the functional relationship for the arched labyrinth weir as shown in Equation (2).

$$C_d = f\left(\frac{h}{H}, F_r, R_e\right) \quad (2)$$

Since the Reynolds number ($R_e = (\rho\ V B)/\mu$) is large in the channel (turbulent flow), the effects of the Reynold's number have been found to be negligible and hence it was omitted from Equation (2) (Azimi et al., 2017; Ebtehaj et al., 2015; Ramamurthy et al., 1986). Therefore, the relationship for the coefficient of discharge, C_d was obtained as Equation (3).

$$C_d = f\left(h/H, F_r\right) \quad (3)$$

To see the effect of various geometric and flow parameters on C_d, and to establish the relationship between the dependent and independent parameters of Equation (3), experiments were carried out in the present study. The methodology adopted in the present study is elaborated in a flowchart as shown in Fig. 1.

P-ISSN: 3050-9734
E-ISSN: 3050-9742
EUROPEAN ADVANCED JOURNAL FOR EMERGING TECHNOLOGIES
EAJET
VOLUME: 03 ISSUE: 03
RECEIVED: APRIL 21 REVISED: MAY 19 ACCEPTED: JUNE 28 PUBLISHED: JULY 11

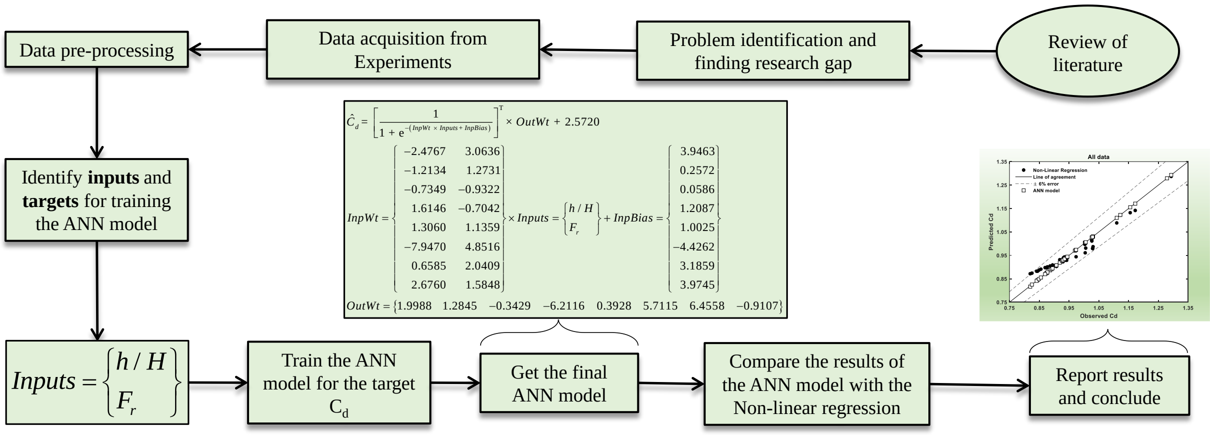

Fig. 1. Methodology flowchart

3. Experimental set-up and procedure

The setup consisted of a channel of 8.0 m length, 0.5 m width and 0.45 m depth. An arched labyrinth weir was provided at 8.5 m from the inlet sump in the channel. Water was supplied to the main channel through an inlet pipe. A rectangular, sharp-crested weir was provided at the end of the channel to measure the discharge flowing through the arched labyrinth weir. Flow suppressors were provided at the channel's entrance to dissipate from the surface disturbances. The present study used an arched labyrinth weir with one notch for experimental purposes. The projected dimension of the notch was 10 cm. The experiment was carried out in free-flow conditions. Depth was measured with a point gauge of 0.1 mm accuracy at 40 cm upstream of the arched labyrinth weir position to avoid the curvature effect of the water surface. The crest heights of the arched labyrinth weir were 18 cm, 20 cm, and 22 cm. The schematic view of the experimental setup is shown in Fig. 2 (Ansari et al., 2021).

P-ISSN: 3050-9734
E-ISSN: 3050-9742
EUROPEAN ADVANCED JOURNAL FOR EMERGING TECHNOLOGIES
EAJET
VOLUME: 03 ISSUE: 03
RECEIVED: APRIL 21 REVISED: MAY 19 ACCEPTED: JUNE 28 PUBLISHED: JULY 11

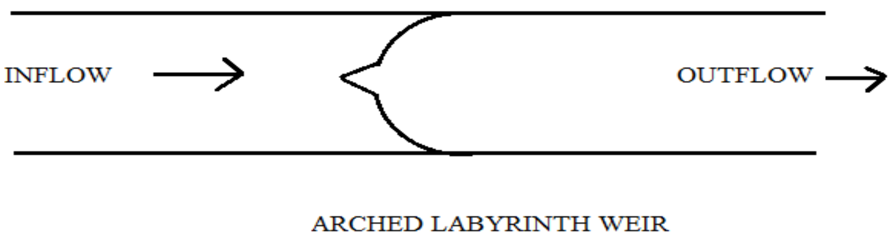

Fig. 2 Plan of experimental setup

Table 1. Data statistics

Parameters	h/H	F_r	C_d	Q
Minimum	0.046	0.010	0.820	0.002
Maximum	0.306	0.100	1.293	0.018
Mean	0.168	0.050	0.965	0.009
Standard deviation, σ	0.071	0.024	0.113	0.005
Mean absolute deviation (MAD)	0.059	0.020	0.086	0.004
Coefficient of variation (Cov)	0.424	0.489	0.117	0.509

The preprocessing of data was performed using Equations (4)-(7) and the results are reported in Table 1. The normalization of the entire experimental dataset was performed using Equation (8).

$$\overline{x} = \sum_{i=1}^{N} \left(\frac{x_i}{N} \right) \tag{4}$$

P-ISSN: 3050-9734 E-ISSN: 3050-9742
EUROPEAN ADVANCED JOURNAL FOR EMERGING TECHNOLOGIES
EAJET
VOLUME: 03 ISSUE: 03
RECEIVED: APRIL 21 REVISED: MAY 19 ACCEPTED: JUNE 28 PUBLISHED: JULY 11

$$\sigma(x) = \sqrt{\left(\frac{1}{N-1}\right)\sum_{i=1}^{N}(x_i - \bar{x})^2} \tag{5}$$

$$MAD(x) = \frac{1}{N}\sum_{i=1}^{N}\left|x_i - \sum_{j=1}^{N}\left(\frac{x_j}{N}\right)\right| \tag{6}$$

$$Cov(x) = \frac{\sigma(x)}{\bar{x}} \tag{7}$$

$$x_N = x_L + \frac{(x_U - x_L)(x - x_{minimum})}{(x_{maximum} - x_{minimum})} \tag{8}$$

Where, x_i and $\hat{x}_i$ denotes the observed and predicted values of the parameters in the dataset, and $\bar{x}$ is its mean. x_N denotes the normalised dataset having minimum ($x_{minimum}$) and maximum ($x_{maximum}$) values as shown in Table 1. The lower and upper bounds are $x_L = 0.1$ and $x_U = 0.9$, respectively.

4. Development of ANN model

Artificial Neural Networks (ANNs) have been extensively utilized in addressing complex nonlinear real-world problems. The development of an ANN requires a minimum of three layers: an input layer, a hidden layer, and an output layer. The network acquires knowledge by identifying patterns and relationships within the data. The input layer receives raw data, which is subsequently processed and transmitted to the hidden layer. The hidden layer further refines the information before passing it to the output layer, where the result is generated. Existing literature highlights the use of various algorithms to optimize the training process of ANNs. Among these, the Levenberg–Marquardt (LM) algorithm is one of the most employed due to its efficiency in training neural networks (Ayaz et al., 2023; Hornik et al., 1989).

In this study, 70% of the total 42 experimental data points from the dataset (refer to Table 1) were randomly partitioned into a training set and 15% of the data was divided into each

P-ISSN: 3050-9734 E-ISSN: 3050-9742
EUROPEAN ADVANCED JOURNAL FOR EMERGING TECHNOLOGIES
EAJET
VOLUME: 03 ISSUE: 03
RECEIVED: APRIL 21 REVISED: MAY 19 ACCEPTED: JUNE 28 PUBLISHED: JULY 11

validation and testing dataset. Subsequently, a neural network architecture comprising an input layer, a single hidden layer, and an output layer was created. The input parameters were selected as *h/H* and F_r to predict the coefficient of discharge (C_d). The optimal size of the hidden layer, indicative of the number of neurons, was determined to achieve better neural network performance. A feed-forward backpropagation (FFBP) network with a single hidden layer was initialized, employing the Levenberg-Marquardt (LM) algorithm for training. Throughout this process, the mean absolute percentage error (MAPE), Mean squared error (MSE), and correlation coefficient (R) were recorded as the hidden layer size was incrementally varied up to 15 neurons. The graphical representation depicted in Fig. 2-4 showcased the variation of MAPE, MSE, and R concerning the number of neurons in the hidden layer across training, validation, and testing datasets. The performance parameters viz. MAPE, MSE and R were calculated using Equations (9)-(11) (Ayaz and Danish, 2025). A clear trend was observed in the model's performance, where MAPE initially decreased with an increasing number of neurons, reaching an optimal value of 0.000258 at a hidden layer size of 8, as illustrated in Fig. 3. Beyond this point, further increases in the number of neurons resulted in negligible improvements in the ANN model's performance, indicating the saturation of its learning capacity. A similar pattern was observed for MSE as shown in Fig. 4, with optimal performance achieved at a hidden layer size of 8 at MSE = 8.0747×10^{-9}. Moreover, the correlation coefficient peaked at R = 1 for a hidden layer size of 8, demonstrating the highest predictive accuracy as shown in Fig. 5. Thus, based on these observations, the optimum ANN architecture for further model development was determined to comprise 2-8-1 neurons in the input layer, hidden layer, and output layer, respectively.

$$\mathrm{MAPE}(x) = \frac{1}{N}\sum_{i=1}^{N}\left|\frac{x_i - \hat{x}_i}{x_i}\right| \tag{9}$$

$$MSE(x) = \sum_{i=1}^{N}\left(\frac{(x_i - \hat{x}_i)^2}{N}\right) \tag{10}$$

P-ISSN: 3050-9734
E-ISSN: 3050-9742
EUROPEAN ADVANCED JOURNAL FOR EMERGING TECHNOLOGIES
VOLUME: 03 ISSUE: 03
RECEIVED: APRIL 21 REVISED: MAY 19 ACCEPTED: JUNE 28 PUBLISHED: JULY 11

$$R(x)=\frac{N\sum_{i=1}^{N}(x_i)(\hat{x}_i)-\left(\sum_{i=1}^{N}x_i\right)\left(\sum_{i=1}^{N}\hat{x}_i\right)}{\sqrt{\left[N\sum_{i=1}^{N}(x_i)^2-\left(\sum_{i=1}^{N}x_i\right)^2\right]\left[N\sum_{i=1}^{N}(\hat{x}_i)^2-\left(\sum_{i=1}^{N}\hat{x}_i\right)^2\right]}} \tag{11}$$

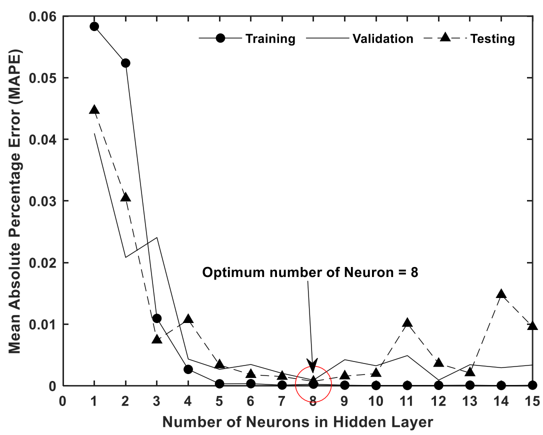

Fig. 3 MAPE versus number of neurons in hidden layer

P-ISSN: 3050-9734
E-ISSN: 3050-9742
EUROPEAN ADVANCED JOURNAL FOR EMERGING TECHNOLOGIES
EAJET
VOLUME: 03 ISSUE: 03
RECEIVED: APRIL 21 REVISED: MAY 19 ACCEPTED: JUNE 28 PUBLISHED: JULY 11

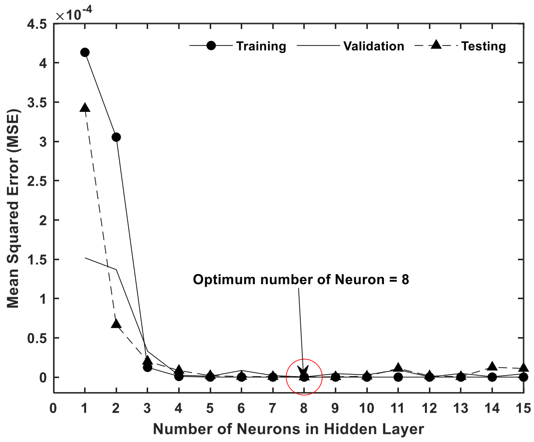

Fig. 4 MSE versus number of neurons in hidden layer

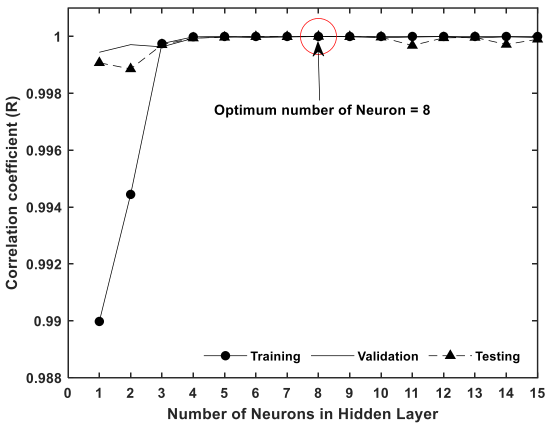

Fig. 5 R versus number of neurons in hidden layer

5. Discussion of results

The non-linear regression analysis was performed using the entire dataset to compare the performance of the ANN model developed in this study. The performance parameters obtained for the developed ANN model for each training, validation and testing datasets are summarized in Table 2. The comparison of the predicted values of coefficient of discharge (C_d) and

P-ISSN: 3050-9734
E-ISSN: 3050-9742
EUROPEAN ADVANCED JOURNAL FOR EMERGING TECHNOLOGIES
EAJET
VOLUME: 03 ISSUE: 03
RECEIVED: APRIL 21 REVISED: MAY 19 ACCEPTED: JUNE 28 PUBLISHED: JULY 11

discharge (Q) are presented in Table 3. The ANN model presented in this study has MSE of 8.07×10^{-9}, 5.48×10^{-6}, and 1.50×10^{-7} for training, validation and testing respectively. Additionally, the MAPE of the ANN model for training validation and testing are 0.000258, 0.009702, and 0.001159, respectively. The lower values of both MSE and MAPE clearly indicate that the ANN model can predict the coefficient of discharge more precisely with the R ≈ 1. Subsequently, the discharge was predicted using the values of C_d (MSE = 2.84×10^{-7}, MAPE = 0.000191) obtained from the ANN model for all data has MSE = $8.97 \times 10^{-11}$and R ≈ 1 respectively. Fig. 6 Shows the regression plot of observed versus predicted coefficient of discharge of ANN model for all, training, validation, and testing data.

The non-linear regression equation of the coefficient of discharge (C_d) is presented in Equation (12). The mathematical representation of the developed ANN model with the input and output weights and values of biases are shown in Equation (13).

$$C_d = 0.290109\left(\frac{h}{H}\right)^{-4.24476} F_r^{\,3.82321} \tag{12}$$

$$\hat{C}_d = \left[\frac{1}{1 + e^{-(InpWt \times Inputs + InpBias)}}\right]^{\mathrm{T}} \times OutWt + 2.5720 \tag{13}$$

$$InpWt = \begin{Bmatrix} -2.4767 & 3.0636 \\ -1.2134 & 1.2731 \\ -0.7349 & -0.9322 \\ 1.6146 & -0.7042 \\ 1.3060 & 1.1359 \\ -7.9470 & 4.8516 \\ 0.6585 & 2.0409 \\ 2.6760 & 1.5848 \end{Bmatrix} \times Inputs = \begin{Bmatrix} h/H \\ F_r \end{Bmatrix} + InpBias = \begin{Bmatrix} 3.9463 \\ 0.2572 \\ 0.0586 \\ 1.2087 \\ 1.0025 \\ -4.4262 \\ 3.1859 \\ 3.9745 \end{Bmatrix}$$

$$OutWt = \{1.9988 \quad 1.2845 \quad -0.3429 \quad -6.2116 \quad 0.3928 \quad 5.7115 \quad 6.4558 \quad -0.9107\}$$

Table 2 Performance evaluation of the developed ANN model

P-ISSN: 3050-9734
E-ISSN: 3050-9742
EUROPEAN ADVANCED JOURNAL FOR EMERGING TECHNOLOGIES
EAJET
VOLUME: 03 ISSUE: 03
RECEIVED: APRIL 21 REVISED: MAY 19 ACCEPTED: JUNE 28 PUBLISHED: JULY 11

Performance parameter	Training	Validation	Testing
MAPE	0.000258	0.009702	0.001159
MSE	8.07×10^{-9}	5.48×10^{-6}	1.50×10^{-7}
R	1.000000	0.999961	0.999994

Table 3 Performance evaluation of ANN model and Non-linear regression

ANN model	**MAPE**	**MSE**	**R**
C_d	0.000191	2.84×10^{-7}	0.999989
Q	0.000191	8.97×10^{-11}	0.999998
Non-linear regression	**MAPE**	**MSE**	**R**
C_d	0.022269	7.71×10^{-4}	0.969495
Q	0.022269	9.66×10^{-8}	0.998815

P-ISSN: 3050-9734 E-ISSN: 3050-9742

EUROPEAN ADVANCED JOURNAL FOR EMERGING TECHNOLOGIES

EAJET

VOLUME: 03 ISSUE: 03

RECEIVED: APRIL 21 REVISED: MAY 19 ACCEPTED: JUNE 28 PUBLISHED: JULY 11

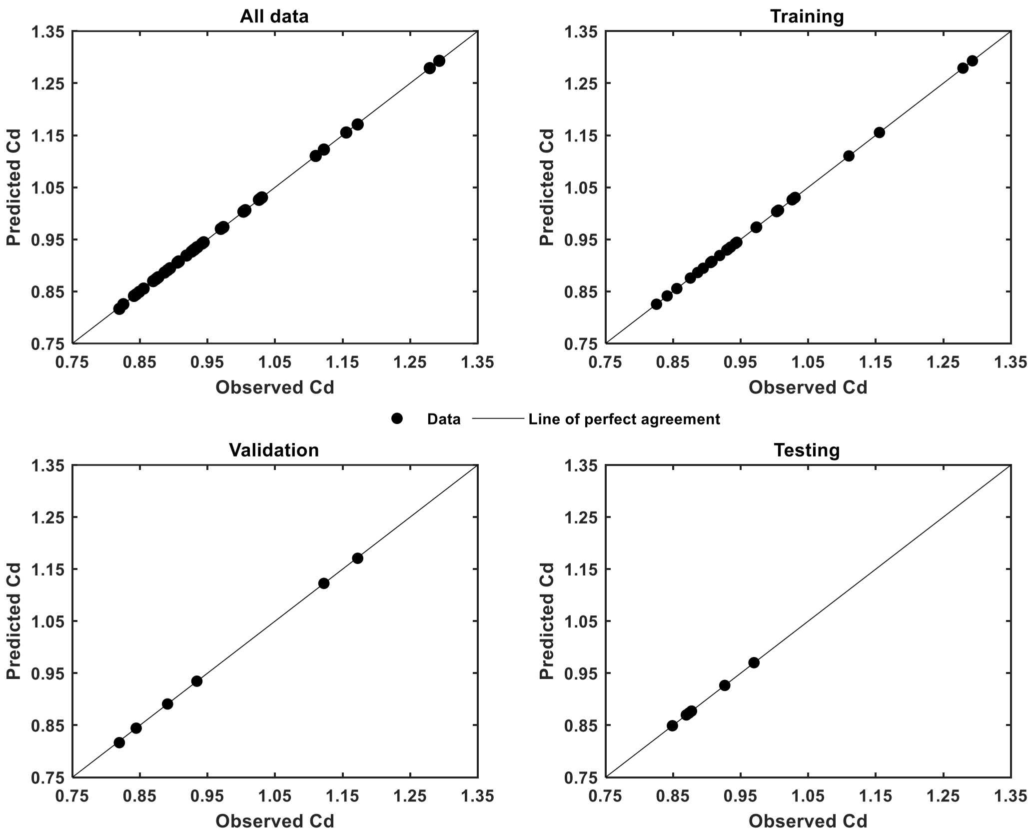

Fig. 6 Regression plot of observed versus predicted coefficient of discharge of ANN model

Comparison of the predicted discharge using Equation (12) and the ANN model is shown in Fig. 7. It is evident from this Fig. that the ANN model accurately predicts coefficient of discharge, since almost all the data points lie on the line of agreement. Moreover, for the non-linear regression Equation (12), the predicted values of coefficient of discharge (MSE = 7.71 $\times 10^{-4}$, MAPE = 0.022269, and R = 0.969) deviated from the line of agreement and lies between the ±6% error line.

P-ISSN: 3050-9734
E-ISSN: 3050-9742
EUROPEAN ADVANCED JOURNAL FOR EMERGING TECHNOLOGIES
EAJET
VOLUME: 03 ISSUE: 03
RECEIVED: APRIL 21 REVISED: MAY 19 ACCEPTED: JUNE 28 PUBLISHED: JULY 11

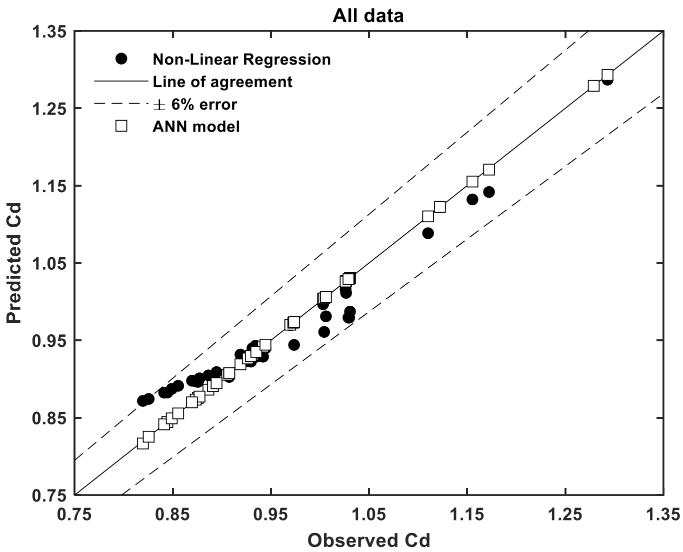

Fig. 7 Comparison of non-linear regression equation and ANN model

5.1.1. *Variation of Discharge coefficient with F_r and h/H*

The variation of coefficient of discharge of arched labyrinth weir with upstream Froude number (F_r) and ratio of water depth over the arched labyrinth weir and height of arched labyrinth weir (h/H) is shown in Fig. 8. It is evident from Fig. 8 that the value of C_d decreases with the increase in Froude number (F_r) and h/H.

P-ISSN: 3050-9734
E-ISSN: 3050-9742
EUROPEAN ADVANCED JOURNAL FOR EMERGING TECHNOLOGIES
EAJET
VOLUME: 03 ISSUE: 03
RECEIVED: APRIL 21 REVISED: MAY 19 ACCEPTED: JUNE 28 PUBLISHED: JULY 11

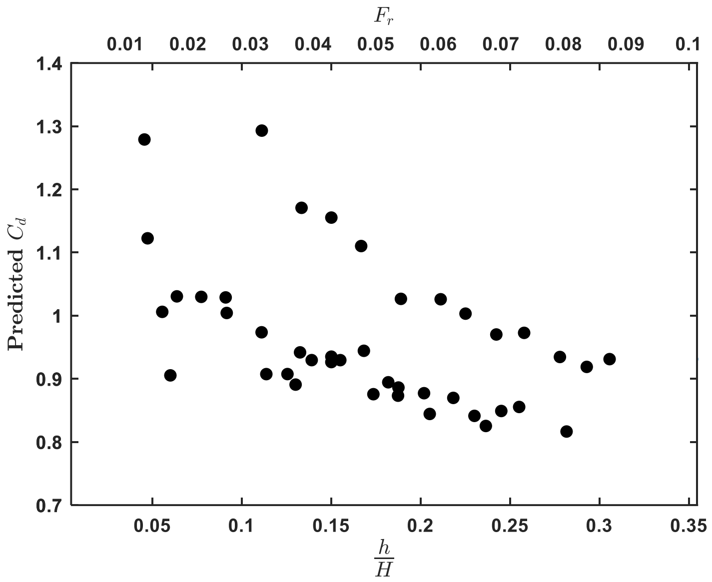

Fig. 8 Variation of C_d with F_r and h/H

6. Conclusion

In this investigation, we conducted experimental analyses to assess an arched labyrinth weir's discharge coefficient (C_d). The observed variation of C_d with the Froude number, (F_r) and the ratio of the upstream head to the weir height (h/H) distinctly illustrates a decline in C_d as F_r and h/H increase. Notably, the Froude number is a crucial parameter in the flow dynamics over arched labyrinth weirs, exerting a noticeable influence on C_d. It has been found that the artificial neural network (ANN) model outperforms the traditional nonlinear regression equation in accurately predicting the coefficient of discharge. Specifically, the ANN model exhibits superior performance metrics with a MSE of 2.84×10^{-7}, MAPE of 0.000191, and a correlation coefficient approximately equal to 1.

Data availability statements

The data used in this study will be available on reasonable request to the corresponding author.

Use of AI tools declaration

The authors declare they have not used Artificial Intelligence (AI) tools in the creation of this article.

P-ISSN: 3050-9734 E-ISSN: 3050-9742

EUROPEAN ADVANCED JOURNAL FOR EMERGING TECHNOLOGIES

EAJET

VOLUME: 03 ISSUE: 03

RECEIVED: APRIL 21 REVISED: MAY 19 ACCEPTED: JUNE 28 PUBLISHED: JULY 11

Conflict of Interest

The authors declare that they have no known competing financial interests or personal relationships that could have appeared to influence the work reported in this paper.

References

1. Amanian, N. (1987). *Performance and design of labyrinth spillway*. 99. https://digitalcommons.usu.edu/etd/7658/
2. Ansari, M. F., Hussain, A., & Ahmad Ansari, M. (2021). Experimental studies and model development of flow over Arched Labyrinth Weirs using GMDH method. *Journal of Applied Water Engineering and Research*, *9*(4), 265–276. https://doi.org/10.1080/23249676.2020.1799443
3. Reddy, V. A. R. (2024). Generative Intelligence for Healthcare Claims Processing and Personalized Benefits Management. International Journal of Advanced Engineering Science and Information Technology (IJAESIT), 7(3), 14099.
4. Ayaz, M., Chourasiya, S., & Danish, M. (2023). Performance analysis of different ANN modelling techniques in discharge prediction of circular side orifice. *Modeling Earth Systems and Environment*. https://doi.org/10.1007/s40808-023-01766-7
5. Azimi, H., Shabanlou, S., Ebtehaj, I., Bonakdari, H., & Kardar, S. (2017). Combination of Computational Fluid Dynamics, Adaptive Neuro-Fuzzy Inference System, and Genetic Algorithm for Predicting Discharge Coefficient of Rectangular Side Orifices. *Journal of Irrigation and Drainage Engineering*, *143*(7). https://doi.org/10.1061/(ASCE)IR.1943-4774.0001190
6. Kolla, S. H. (2024). Retrieval-Augmented Enterprise Intelligence: Enhancing Accuracy, Trust, and Operational Decision-Making. International Journal of Future Innovative Science and Technology (IJFIST), 7(2), 12425.
7. Bilhan, O., & Emiroglu, M. E. (2016). Experimental Studies on Determination of Discharge Capacity of Circular Labyrinth Weirs Located on A Straight Channel. *International Journal of Electronics, Mechanical and Mechatronics Engineering*, *6*, 1227–1239. https://api.semanticscholar.org/CorpusID:62910498
8. Crookston, B. M. (2010). Labyrinth weirs (Ph. D. Dissertation). *Logan: Utah State University Library*, 95–122.
9. Crookston, B. M., Flake, L. K., & Felder, S. (2024). Flow Nonuniformity and Energy Dissipation in Moderate-Sloped Stepped Chutes with a Labyrinth Crest. *Journal of Hydraulic Engineering*, *150*(5). https://doi.org/10.1061/JHEND8.HYENG-13881

P-ISSN: 3050-9734
E-ISSN: 3050-9742
EUROPEAN ADVANCED JOURNAL FOR EMERGING TECHNOLOGIES
EAJET
VOLUME: 03 ISSUE: 03
RECEIVED: APRIL 21 REVISED: MAY 19 ACCEPTED: JUNE 28 PUBLISHED: JULY 11

10. Nagubandi, A. R. (2023). Advanced Multi-Agent AI Systems for Autonomous Reconciliation Across Enterprise Multi-Counterparty Derivatives, Collateral, and Accounting Platforms. International Journal of Finance (IJFIN)-ABDC Journal Quality List, 36(6), 653-674.
11. Crookston, B. M., & Tullis, B. P. (2012). Labyrinth Weirs: Nappe Interference and Local Submergence. *Journal of Irrigation and Drainage Engineering*, *138*(8), 757–765. https://doi.org/10.1061/(ASCE)IR.1943-4774.0000466
12. Crookston, B. M., & Tullis, B. P. (2013). Hydraulic Design and Analysis of Labyrinth Weirs. II: Nappe Aeration, Instability, and Vibration. *Journal of Irrigation and Drainage Engineering*, *139*(5), 371–377. https://doi.org/10.1061/(ASCE)IR.1943-4774.0000553
13. Loganathan, R. (2024). GENERATIVE AI-ENABLED COMPLIANCE DOCUMENTATION AND AUDIT TRAIL AUTOMATION FOR GLOBAL DATA CENTER GOVERNANCE. Turkish Journal of Computer and Mathematics Education (TURCOMAT), 15(3), 487-504.
14. Darvas, L. A. (1971). Discussion of “Performance and Design of Labyrinth Weirs.” *Journal of the Hydraulics Division*, *97*(8), 1246–1251. https://doi.org/10.1061/JYCEAJ.0003056
15. Ebtehaj, I., Bonakdari, H., Khoshbin, F., & Azimi, H. (2015). Pareto genetic design of group method of data handling type neural network for prediction discharge coefficient in rectangular side orifices. *Flow Measurement and Instrumentation*, *41*, 67–74. https://doi.org/10.1016/j.flowmeasinst.2014.10.016
16. Ghodsian, M. (2009). Stage–discharge relationship for a triangular labyrinth spillway. *Proceedings of the Institution of Civil Engineers - Water Management*, *162*(3), 173–178. https://doi.org/10.1680/wama.2009.00033
17. Aitha, A. R. (2021). Dev Ops Driven Digital Transformation: Accelerating Innovation In The Insurance Industry. Available at SSRN 5622190.
18. Hay, N., & Taylor, G. (1970). Performance and Design of Labyrinth Weirs. *Journal of the Hydraulics Division*, *96*(11), 2337–2357. https://doi.org/10.1061/JYCEAJ.0002766
19. Hornik, K., Stinchcombe, M., & White, H. (1989). Multilayer feedforward networks are universal approximators. *Neural Networks*, *2*(5), 359–366. https://doi.org/10.1016/0893-6080(89)90020-8
20. Kolla, S. K. (2024). Clinical Knowledge Intelligence through Deep Learning and Natural Language Understanding in Healthcare Platforms. International Journal of Advanced Engineering Science and Information Technology (IJAESIT), 7(3), 14088.
21. Houston, K. L. (1982). Hydraulic model study of Ute Dam labyrinth spillway. *Report GR-82-7 August 1982. 47 p, 30 Fig, 2 Tab, 4 Ref, 1 Append.*
22. Hussain, R. A., Hassan, S. A., & Jamel, A. A. J. (2022). Experimental Study on Flow over

P-ISSN: 3050-9734
E-ISSN: 3050-9742
EUROPEAN ADVANCED JOURNAL FOR EMERGING TECHNOLOGIES
EAJET
VOLUME: 03 ISSUE: 03
RECEIVED: APRIL 21 REVISED: MAY 19 ACCEPTED: JUNE 28 PUBLISHED: JULY 11

Triangular Labyrinth Weirs. *International Journal of Design & Nature and Ecodynamics*, *17*(2), 249–255. https://doi.org/10.18280/ijdne.170211

23. Idrees, A. K., & Al-Ameri, R. (2022). Improving the performance of the compound labyrinth weirs using an artificial ventilation approach. *Water Supply*, *22*(8), 6585–6602. https://doi.org/10.2166/ws.2022.260
24. Idrees, A. K., & Al-Ameri, R. (2023). Investigation of flow characteristics and energy dissipation over new shape of the trapezoidal labyrinth weirs. *Flow Measurement and Instrumentation*, *89*, 102276. https://doi.org/10.1016/j.flowmeasinst.2022.102276
25. Davuluri, P. N. (2020). Event-Driven Architectures for Real-Time Regulatory Monitoring in Global Banking.
26. Idrees, A. K., Al-Ameri, R., Chua, L. H. C., & Das, S. K. (2018). *Discharge characteristics for trapezoidal compound labyrinth*. https://api.semanticscholar.org/CorpusID:190202605
27. Idrees, A. K., Al-Ameri, R., & Das, S. K. (2016). *Determination of discharge coefficient for flow over one cycle compound trapezoidal plan form labyrinth weir*. https://api.semanticscholar.org/CorpusID:76655879
28. Khode, B. V, & Tembhurkar, A. R. (2010). Evaluation and Analysis of Crest Coefficient for Labyrinth Weir. *World Applied Sciences Journal*, *11*, 835–839. https://api.semanticscholar.org/CorpusID:16856730
29. Lux, F. (1984). Discharge Characteristics of Labyrinth Weirs. *Water for Resource Development*, 385–389. https://api.semanticscholar.org/CorpusID:116591065
30. Ramamurthy, A. S., Tim, U. S., & Sarraf, S. (1986). Rectangular Lateral Orifices in Open Channels. *Journal of Environmental Engineering*, *112*(2), 292–300. https://doi.org/10.1061/(ASCE)0733-9372(1986)112:2(292)
31. Inala, R. Advancing Group Insurance Solutions Through Ai-Enhanced Technology Architectures And Big Data Insights.
32. Sangsefidi, Y., Mehraein, M., & Ghodsian, M. (2018). Experimental study on flow over in-reservoir arced labyrinth weirs. *Flow Measurement and Instrumentation*, *59*, 215–224. https://doi.org/10.1016/j.flowmeasinst.2017.12.002
33. Savage, B. M., Frizell, K. H., & Crowder, J. W. (2004). *Brains versus Brawn : The Changing World of Hydraulic Model Studies*. https://api.semanticscholar.org/CorpusID:46743321
34. Taylor, G. (1968). *The performance of labyrinth weirs*. University of Nottingham Nottingham, England.
35. Tullis, B. P., Young, J. C., & Chandler, M. A. (2007). Head-Discharge Relationships for Submerged Labyrinth Weirs. *Journal of Hydraulic Engineering*, *133*(3), 248–254. https://doi.org/10.1061/(ASCE)0733-9429(2007)133:3(248)

P-ISSN: 3050-9734
E-ISSN: 3050-9742

EUROPEAN ADVANCED JOURNAL FOR EMERGING TECHNOLOGIES

VOLUME: 03 ISSUE: 03

RECEIVED: APRIL 21 REVISED: MAY 19 ACCEPTED: JUNE 28 PUBLISHED: JULY 11

36. Tullis, J. P., Amanian, N., & Waldron, D. (1995). Design of Labyrinth Spillways. *Journal of Hydraulic Engineering*, *121*(3), 247–255. https://doi.org/10.1061/(ASCE)0733-9429(1995)121:3(247)
37. Yousif, O. S. Q., & Karakouzian, M. (2020). Effect of Corner Shape on Hydraulic Performance of One-Cycle Rectangular Labyrinth Weirs. *Fluids*, *5*(3), 117. https://doi.org/10.3390/fluids5030117
38. Md Ayaz; Mohd Danish. [*In Press*]. "Discussion of "A Novel and Enhanced Calibration of the Tilting Weir as a Flow Measurement Structure" by Joseph E. Pugh et al." *Journal of Hydraulic Engineering*. 10.1061/JHEND8/HYENG-14206